

INFLUENCE OF TEMPERING TEMPERATURE ON THE MICROSTRUCTURE AND ULTIMATE TENSILE STRENGTH OF 28Cr3SiNiMoWV STEEL

VPLIV TEMPERATURE POPUŠČANJA NA MIKROSTRUKTURU IN NATEZNO TRDNOST JEKLA VRSTE 28Cr3SiNiMoWV

Minh Ngoc Nguyen^{1*}, Ngan Hanh Vu²

¹School of Materials Science and Engineering, Hanoi University of Science and Technology (HUST), No.1, Dai Co Viet street, Hanoi, Vietnam

²Center of Materials and Failure Analysis, Institute of Materials Science, No. 18, Hoang Quoc Viet, Cau Giay, Hanoi, Vietnam

Prejem rokopisa – received: 2023-02-03; sprejem za objavo – accepted for publication: 2023-08-27

doi:10.17222/mit.2023.787

In this research, the influences of the tempering temperature on the microstructure and ultimate tensile strength of 28Cr3SiNiMoWV steel were studied. The microstructure and ultimate tensile strength were investigated after tempering 28Cr3SiNiMoWV steel at different temperatures, ranging from 280 °C to 440 °C for 2 h. The results show that after tempering it at different temperatures, the microstructure of 28Cr3SiNiMoWV steel was tempered martensite. During the tempering process, the alloy carbides precipitated in the martensite matrix. Precipitation of alloy carbides in the microstructures of different specimens is the cause for an increase in the ultimate tensile strength. With the increasing tempering temperature, the ultimate tensile strength initially increases from 1390 MPa to 1601 MPa, and then decreases to 1466 MPa, with its maximum value at 280 °C.

Keywords: 28Cr3SiNiMoWV steel, ultimate tensile strength, tempering temperature

Povzetek: v pričujočem članku avtorji opisujejo raziskavo vpliva temperature popuščanja na mikrostrukturo in natezno trdnost jekla vrste 28Cr3SiNiMoWV. Mehanske lastnosti in mikrostrukturo preiskovanega jekla so določili po kaljenju pri 920 °C in po dvehurnem popuščanju pri temperaturah med 280 °C in 440 °C. Po popuščanju je v vseh primerih jeklo imelo mikrostrukturo popuščene martenzite. Med popuščanjem so se z naraščajočo temperaturo popuščanja iz martenzite matrice izločali ustrezno veliki karbidni izločki zlitinskih elementov, kar je povzročilo proporcionalno spremembo natezne trdnosti jekla. V izhodnem stanju je imelo preiskovano jeklo natezno trdnost 1390 MPa. Pri najnižji izbrani temperaturi popuščanja 280 °C je imelo jeklo najvišjo natezno trdnost 1601 MPa in pri najvišji temperaturi popuščanja 440 °C najnižjo natezno trdnost 1466 MPa.

Ključne besede: jeklo vrste 28Cr3SiNiMoWV, natezna trdnost, temperatura popuščanja

1 INTRODUCTION

High-strength steel has been widely used for producing landing gear, high stress joints, wing beams and bolts in the aviation industry because of its many distinguished advantages, such as high strength, high hardness, good fracture toughness, etc. In order to obtain these advantages, steel needs to have an appropriate microstructure. In recent years, many studies on the control of steel microstructures were carried out by researchers. Related research on, for example, the grain size control^{1,2}, control of carbide precipitation within a very small range,³ twin martensite effect,^{4,5} control of the phase ratio by a heat treatment process,^{6,7} etc., was done. Although many important discoveries have been made, the microcosmic understanding of different steel types is still in the process of continuous development. Especially the studies on the precipitation of alloy carbides in tempered martensite under heat treatment conditions still attract a lot of attention from researchers.^{8,9} This is be-

cause an addition of certain alloying elements to a composition can improve the mechanical properties of steel, but the production cost increases. In order for the required properties of steel to be obtained, the most economical and suitable steel type should be selected. Heat treatment is one of the most economical and feasible methods for adjusting the mechanical properties.¹⁰ This method, consisting of quenching and tempering, is known as the most common application in mechanical manufacturing. It helps to create fine carbide particles during a tempering process, providing a major strengthening effect in many steel types.¹¹ For this purpose, the tempering treatment is an important necessary stage for improving the ultimate tensile strength (UTS) of steel. However, the tempering temperature range allowing the suitable precipitation of alloy carbides often depends on the chemical composition of individual steels.¹² Therefore, it is necessary to study and optimize specific temperature ranges, thereby optimizing the mechanical properties of steel.

In this study, the effects of the tempering temperatures of 280–440 °C on the microstructure and UTS of 28Cr3SiNiMoWV steel are discussed. The aim of this

*Corresponding author's e-mail:
minh.nguyennoc@hust.edu.vn (Minh Ngoc Nguyen)

study is to select the best tempering temperature range allowing a significant increase in the UTS of 28Cr3SiNiMoWV steel.

2 EXPERIMENTAL PART

The chemical composition of the 28Cr3SiNiMoWV steel was analysed using a SPECTROMAXx (SPECTRO, LMX10). Samples for the microstructural analysis were prepared, having a cubic shape and dimensions of (10 × 10 × 10) mm while samples for the tensile testing were made according to the ISO 7500-1 standard. All the samples were quenched in an oil quenching medium before being subjected to next tempering stage. In order to select the appropriate quenching temperature, the Thermo-Calc program (Thermo-Calc, 2015b, TCFE7) was used to calculate and build the phase diagram for the steel composition shown in **Table 1**.

Table 1: Chemical composition of the 28Cr3SiNiMoWV steel

Element	C	Si	Cr	Ni	Mo	Mn	W	V	P	S	Fe
w/%	0.29	0.95	2.83	1.01	0.35	0.56	0.81	0.06	0.01	0.01	Bal.

The binary diagram is shown in **Figure 1**. The selection of the quenching temperature based on the phase diagram must ensure that the microstructure of the steel is completely austenitic before cooling. However, the temperature should not be too high so that the fine austenite grains can be maintained. For this reason, the quenching temperature was selected to be 920 °C. To evaluate the effect of the tempering temperature, the quenched samples were tempered at (280, 360 and 440) °C for 2 h be-

fore the microstructural observation and tensile testing. All sample surfaces were protected to prevent oxidation and decarburization during heat treatment processes.

For the observation and evaluation of the microstructure, the cubic samples were cross-sectioned, ground, polished and etched by the Vilella solution before a scanning electron microscope coupled with an energy-dispersive spectrometer (SEM, JEOL JSM-6500F, EDS INCA X-SIGHT LH2-type detector, INCA ENERGY 450) was used to analyse the chemical compositions of the phases. In addition, the crystal structures of the phases were also characterized with X-ray diffraction (XRD, ARL EQUINOX 5000), with the Cu K_{α} radiation operating at 60 kV, 60 mA. The measurements were recorded in a 2θ range of 20–90° at a scanning speed of 2° per min and a 2θ step of 0.015°.

The values of the UTS were determined using a tensile testing machine (WE-1000B, New Luda). Before the tensile tests of the specimens, the surfaces of the samples were cleaned to obtain effective cross-sections and precise residual mechanical properties. The tensile tests were conducted at room temperature using a 500 kN load cell with a displacement rate of 2 mm/min. The tests were recorded by the software, which automatically calculated the data.

3 RESULTS AND DISCUSSION

The microstructures of the as-received, quenched and tempered samples are shown in **Figure 2**. In the as-received sample (**Figure 2a**), the shape of the crystal grains is slightly flattened in a certain direction. This in-

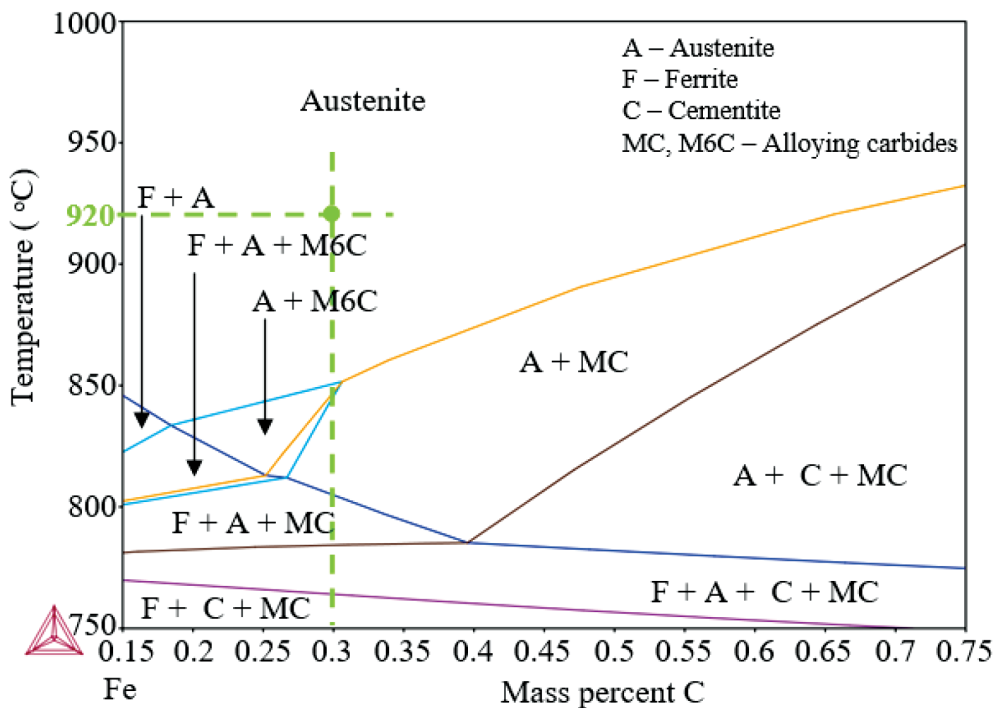


Figure 1: Phase diagram of the 28Cr3SiNiMoWV steel calculated using Thermocalc software

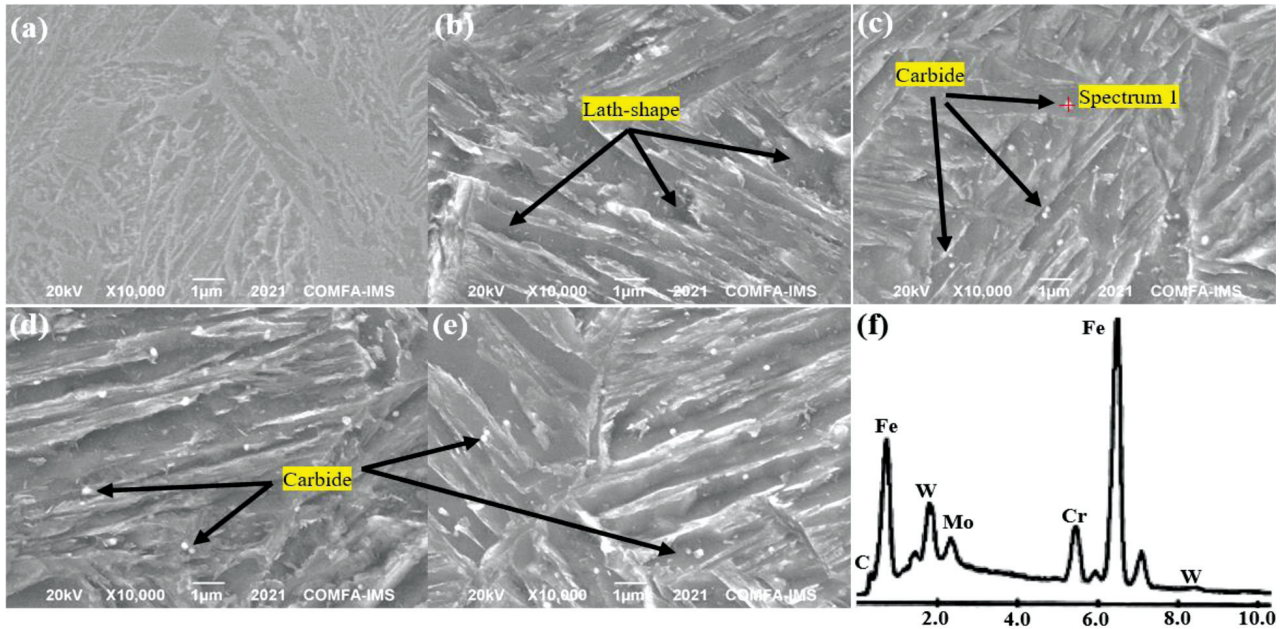


Figure 2: SEM images and EDS analysis of the samples: a) as-received, b) quenched, c) quenched and tempered at 280 °C, d) quenched and tempered at 360 °C, e) quenched and tempered at 440 °C, f) EDS result of spectrum 1

indicates that the used steel has probably undergone a previous hot rolling process. **Figure 2b** shows a fully martensitic structure of the quenched sample with lath-shaped features.¹³ This proves that the quenched temperature and quenching medium selected above are completely suitable. In the tempered samples (**Figures 2c to 2e**), the tempered martensite was obtained through tempering in a temperature range of 280–440 °C. The tempered martensite was similar to that of the quenched sample, but the difference was that there was precipitation of the fine spherical carbides in the lath regions after the tempering, as shown by the black arrows (**Figures 2c to 2e**). In addition, it can also be seen that the particle size of carbides in the sample tempered at a low temperature (**Figure 2c**) is smaller than in the sample tempered at a higher temperature (**Figure 2e**). This is because with an increase in the tempering temperature, martensite decomposed faster, allowing carbon and alloying atoms to move out of the martensite easily to form carbides. This led to an increase in the particle size of carbides. **Figure 2f** shows the EDS result for the alloy carbide particle distribution in the tempered-martensite matrix.

Figure 3 shows X-ray diffraction patterns of the samples, and the presence of the highest intensity peaks related to the ferrite phase (the as-received sample) and martensite phase (quenched, tempered samples). A comparison between the position of the main peak of the as-received sample (**Figure 3a**) and the main peak of the quenched sample (**Figure 3b**) shows that the latter tends to shift to the left in the direction of a smaller 2θ angle. This is because during the austenitizing process, carbon and alloying elements were more soluble in the solid so-

lution. Thereby, the lattice constant was increased, resulting in a decrease in the 2θ angle.

For all of the tempered samples (**Figures 3c to 3e**), the tendency to shift the positions of the main diffraction peaks occurs in the opposite direction. At the higher tempering temperature (**Figure 3e**), the 2θ angle shifts more to the right, with a larger diffraction angle. This is due to the fact that at a higher tempering temperature, the decomposition rate of quenched martensite is faster. This reduces the lattice constant, resulting in an increase in the 2θ diffraction angle. No diffraction peaks of the alloy carbide were observed. This may be because the density of the carbide particles is not high and the size of the car-

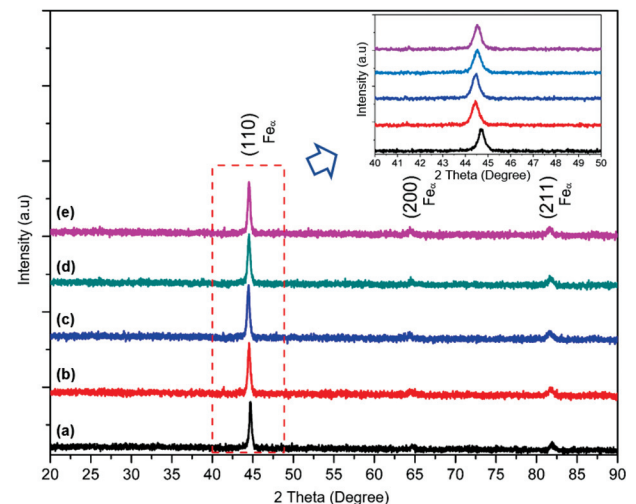


Figure 3: XRD patterns of the samples: a) as-received, b) quenched, c) quenched and tempered at 280 °C, d) quenched and tempered at 360 °C, (e) quenched and tempered at 440 °C

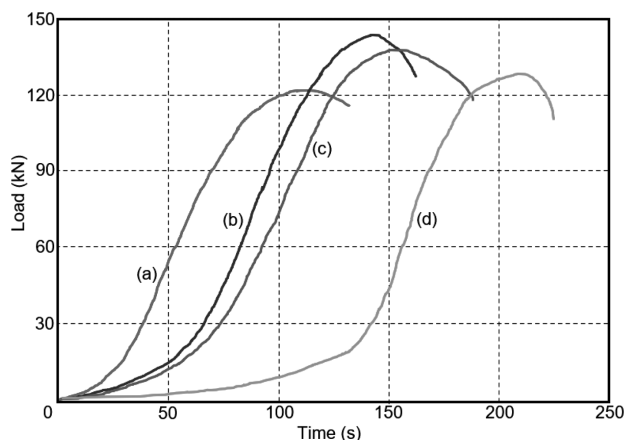


Figure 4: Load-time record for the tensile test: a) as-received – sample a, b) quenched and tempered at 280 °C – sample b, c) quenched and tempered at 360 °C – sample c, d) quenched and tempered at 440 °C – sample d

bide particles is very small, so it is difficult to recognize XRD. Thus, the types of the alloy carbides could not be detected with XRD measurements due to their small size and low content. However, based on the alloy composition (Table 1), the tempering temperatures and the phase diagram shown in **Figure 1**, it is possible to predict that the alloy carbides are in the forms of MC and M₃C (cementite).

Figure 4 shows the load-time relationship for the tensile test, and the UTS of the samples is shown in **Table 2**. The UTS values for the samples after tempering (**Figures 4b to 4d**) are increased in comparison with the as-received sample (**Figure 4a**), proving that the precipitation of alloy carbides during the tempering process improves the UTS of the steel. However, with an increase in the tempering temperature, the tempered martensite is quickly further decomposed into ferrite and carbides. Compared with the tempering at a lower temperature, the carbides that precipitate on the matrix become bigger and coarser. In addition, the recovery rate of the matrix increases significantly, making the dislocation density decrease. All of these developments reduce the UTS of the steel.

Table 2: Ultimate tensile strength values for the samples

Type of sample	Sample a	Sample b	Sample c	Sample d
UTS (MPa)	1390	1601	1570	1466

4 CONCLUSIONS

The tempering temperature can be used to control the microstructure and ultimate tensile strength of 28Cr3SiNiMoWV steel. In a tempering temperature range of 280–440 °C, with an increase in the tempering temperature, the tempered martensite was quickly further decomposed into ferrite and carbides while the ultimate

tensile strength showed a decreasing trend. The highest value of the ultimate tensile strength was 1601 MPa, corresponding to a tempering temperature of 280 °C.

Acknowledgment

This research was funded by the Hanoi University of Science and Technology (HUST) under project number T2022-PC-084.

5 REFERENCES

- L. Lan, C. Qiu, L. Du, Effective grain size dependence of crack propagation resistance in low carbon steel, *Theor. Appl. Fract. Mech.*, 124 (2023), 103762, doi:10.1016/j.tafmec.2023.103762
- M. Diao, C. Guo, Q. Sun, F. Jiang, L. Li, J. Li, D. Xu, C. Liu, H. Song, Improving mechanical properties of austenitic stainless steel by the grain refinement in wire and arc additive manufacturing assisted with ultrasonic impact treatment, *Mater. Sci. Eng. A*, 857 (2022), 144044, doi:10.1016/j.msea.2022.144044
- Ø. Grong, L. Kolbeinsen, C. V. D. Eijk, G. Tranell, Microstructure Control of Steels through Dispersoid Metallurgy Using Novel Grain Refining Alloys, *ISIJ International*, 46 (2006) 6, 824–31, doi:10.2355/isijinternational.46.824
- P. Zhang, Y. Chen, W. Xiao, D. Ping, X. Zhao, Twin structure of the lath martensite in low carbon steel, *Pro. in Nat. Sci.: Mat. Int.*, 26 (2016) 2, 169–72, doi:10.1016/j.pnsc.2016.03.004
- J. W. Liu, X. Luo, B. Huang, Y. Q. Yang, W. J. Lu, X. W. Yi, H. Wang, Nano-Twinning and Martensitic Transformation Behaviors in 316L Austenitic Stainless Steel During Large Tensile Deformation, *Acta Metall. Sin.*, 36 (2022), doi:10.1007/s40195-022-01487-3
- E. Olorundaisi, T. Jamiru, T. A. Adegbola, Response surface modeling and optimization of temperature and holding time on dual phase steel, *Materials Today: Proceedings*, 38 (2021) 2, 1164–69, doi:10.1016/j.matpr.2020.07.408
- D. Frómota, N. Cuadrado, J. Rehrl, C. Suppan, T. Dieudonné, P. Dietsch, J. Calvo, D. Casellas, Microstructural effects on fracture toughness of ultra-high strength dual phase sheet steels, *Mater. Sci. Eng. A*, 802 (2021), 140631, doi:10.1016/j.msea.2020.140631
- Y. Zheng, F. Wang, C. Li, Y. Lin, R. Cao, Effect of Martensite Structure and Carbide Precipitates on Mechanical Properties of Cr-Mo Alloy Steel with Different Cooling Rate, *High Temp. Mater. Proc.*, 38 (2019), 113–24, doi:10.1515/htmp-2018-0018
- T. Zhou, R. P. Babu, Z. Hou, J. Odqvist, P. Hedström, Precipitation of multiple carbides in martensitic CrMoV steels - experimental analysis and exploration of alloying strategy through thermodynamic calculations, *Materialia*, 9 (2020), 100630, doi:10.1016/j.mtla.2020.100630
- X. Yao, J. Huang, Y. Qiao, M. Sun, B. Wang, B. Xu, Precipitation Behavior of Carbides and its Effect on the Microstructure and Mechanical Properties of 15CrNi3MoV Steel, *Metals*, 12 (2022) 10, 1758, doi:10.3390/met12101758
- S. H. Talebi, M. Jahazi, H. Melkonyan, Retained Austenite Decomposition and Carbide Precipitation during Isothermal Tempering of a Medium-Carbon Low-Alloy Bainitic Steel, *Materials (Basel)*, 11 (2018) 8, 1441, doi:10.3390/ma11081441
- S. A. Yamini, Influence of microalloying elements (Ti, Nb) and nitrogen concentrations on precipitation of pipeline steels – A thermodynamic approach, *Engineering Reports*, 3 (2020) 7, 1–10, doi:10.1002/eng2.12337
- M. M. A. Bepari, Carburizing: A Method of Case Hardening of Steel, *Comp. Mat. Fin.*, 2 (2017), 71–106, doi:10.1016/B978-0-12-803581-8.09187-6